TU Delft

Delft University of Technology

Document Version
Final published version

Licence
Dutch Copyright Act (Article 25fa)

Citation (APA)
Ranaweera, D., Zafari, B., Overend, M., & Peiris, D. (2026). Flexural Response of Glass-GFRP Composite Sandwich Façade Panels. In J. Sena-Cruz, J. A. O. Barros, L. Correia, J. Custódio, & A. S. Louro (Eds.), *12th International Conference on FRP Composites in Civil Engineering, CICE 2025 - Volume 2* (pp. 81-90). (Lecture Notes in Civil Engineering; Vol. 778 LNCE). Springer. https://doi.org/10.1007/978-3-032-09387-5_9

Important note
To cite this publication, please use the final published version (if applicable).
Please check the document version above.

Copyright
In case the licence states “Dutch Copyright Act (Article 25fa)”, this publication was made available Green Open Access via the TU Delft Institutional Repository pursuant to Dutch Copyright Act (Article 25fa, the Taverne amendment). This provision does not affect copyright ownership.
Unless copyright is transferred by contract or statute, it remains with the copyright holder.

Sharing and reuse
Other than for strictly personal use, it is not permitted to download, forward or distribute the text or part of it, without the consent of the author(s) and/or copyright holder(s), unless the work is under an open content license such as Creative Commons.

Takedown policy
Please contact us and provide details if you believe this document breaches copyrights.
We will remove access to the work immediately and investigate your claim.

This work is downloaded from Delft University of Technology.

Flexural Response of Glass-GFRP Composite Sandwich Façade Panels

D. Ranaweera[1(✉)], B. Zafari[1], M. Overend[2], and D. Peiris[1]

[1] Faculty of Engineering, Computing and the Environment, Kingston University London, London, UK
{K1464166,B.Zafari}@kingston.ac.uk
[2] Department of Architectural Engineering + Technology, TU Delft, Delft, Netherlands
M.Overend@tudelft.nl

Abstract. This study addresses the limited understanding of the structural performance of composite sandwich façade panels made with glass and pultruded glass fiber-reinforced polymer (GFRP), which represent a promising alternative to conventional aluminum glazed systems. These panels, measuring 1300 × 600 mm, were experimentally tested under monotonic flexural loading to explore the influence of adhesive type on structural performance, comparing assemblies bonded with silicone-based adhesives to those bonded with epoxy-based adhesives. An initial-stage ANSYS FE model was developed and validated against the experimental results, providing further confidence in the findings and enabling predictive analysis. Key focus areas include analyzing the flexural response and investigating shear lag effects, which are critical to understanding the effective widths and mechanical behavior of glazed composite sandwich panels. The findings highlight that epoxy-bonded panels demonstrate significantly greater stiffness and load-bearing capacity compared to silicone-bonded panels, underscoring the importance of adhesive properties in achieving optimal performance. This research contributes to the development of analytical models that can accurately predict the behavior of glass-GFRP composite panels, providing engineers and designers with essential insights into the mechanical performance of such systems. By demonstrating the feasibility of replacing traditional aluminum unitized curtain walls with glass-GFRP sandwich panels, this study illustrates the potential to create slimmer, stronger, and more durable façade systems with enhanced corrosion resistance. These findings support the transformative role of composite materials in advancing façade panel design for minimalist, sustainable, and architecturally innovative building exteriors.

Keywords: Façade · Sandwich Structures · Adhesively Bonded Connections · GFRP · Façade Panels · Glass

1 Introduction

The increasing emphasis on energy efficiency and minimalistic aesthetic appeal in architectural design has driven advancements in building façade technologies. Traditional non-composite glazed curtain wall systems, typically constructed with aluminum

© The Author(s), under exclusive license to Springer Nature Switzerland AG 2026
J. Sena-Cruz et al. (Eds.): CICE 2025, LNCE 778, pp. 81–90, 2026.
https://doi.org/10.1007/978-3-032-09387-5_9

frames either mechanically fastened or adhesively bonded to glazing panels, exhibit limited composite action. This lack of integration reduces material efficiency, necessitating larger frame sections and constraining span capabilities. Consequently, there is a growing demand for lightweight, structurally efficient, and aesthetically versatile façade systems. In response, adhesively bonded composite glazing façade panels have emerged as a promising solution, offering the potential to enhance composite action under flexural loads and achieve superior structural performance compared to conventional aluminum-glass systems.

The concept of utilizing composite structures involving glass and materials such as metals, timber, or fiber-reinforced polymers (FRPs) has been extensively investigated in prior research, particularly through structural testing of composite beams materials [1, 2]. While many studies have focused on metal-based components either mechanically fastened or adhesively bonded to glass panels, significant progress has not been made in understanding the potential of FRP-based composites with glass. Pascual et al. [3] explored adhesively bonded glass-GFRP sandwich beams, experimentally characterizing their behavior under monotonic loading and developing analytical and numerical predictive models for their structural performance. Further research conducted by the authors of this study [4] examined the flexural behavior of adhesively bonded glass-GFRP composite beams under sustained loading conditions.

The investigation of composite edge-framed glazed facade panels has gained attention in recent years. Medium-scale glass-steel composite glazing panels bonded using epoxy-based adhesives such as Araldite 2047 have demonstrated superior performance, achieving more than twice the ultimate failure load and less than half the mid-span deflections of their unbonded counterparts [5]. Additionally, research conducted by Pascual et al. [6] on large-scale composite panels has shown up to 90% composite action under structural loads. However, these studies have predominantly focused on metallic edge frames. While metal-based edge frames contribute to structural efficiency, they also present challenges, such as differential thermal expansion to the glass face sheets, which can lead to internal stresses and potential long-term performance issues.

Building on these findings, the use of pultruded GFRP edge frames in composite glazing panels emerges as an innovative alternative that remains largely unexplored. GFRP edge frames offer unique benefits, including superior thermal insulation compared to traditional glass-metal systems, making them particularly advantageous for energy-efficient building designs [7]. This study aims to bridge this research gap by experimentally and numerically investigating the structural performance of medium-scale GFRP-glass composite unitized curtain wall panels. Through this work, we seek to provide a comprehensive understanding of their flexural behavior and demonstrate their potential to enhance façade technology with improved strength, aesthetics, thermal and acoustic performance.

2 Specimen Configurations and Experimental Setup

2.1 Material Properties

Four medium scaled specimens were fabricated for this study, each featuring distinct cross-sectional configurations arising from variations in material combinations and adhesive types. The specimens were manufactured using two fully toughened (FT) and/or toughened laminated glass face sheets adhesively bonded to a structural core made of aluminum or GFRP SHS profiles. Two different adhesive types, 3M DP490 (epoxy) and DC995 (silicone) were employed. The specimen configuration of each specimen is explained below in Sect. 2.2. Material properties for all components were determined through material testing and supplemented with data from literature.

Table 1. Material properties

Material Property	GFRP core full section	Aluminum core [8]	3M DP490 adhesive [3]	DC995 Adhesive [9]	FT glass face sheet [8]
E_x (GPa)	26.9	69	135 e^{-3}	1.38 e^{-3}	72
E_y (GPa)	10.1				
E_z (GPa)	10.1				
G_{xy} (GPa)	3.2	25.5	49 e^{-3}	29.5 e^{-3}	29
G_{xz} (GPa)	3.2				
G_{yz} (GPa)	2.6				

To characterize the material properties of the pultruded GFRP core, burn-off tests were conducted in accordance with ASTM D3171-11 [10]. A total of four specimens, extracted from the pultruded GFRP core, were tested to determine material properties along all three principal axes. Two configurations were prepared for each GFRP profile: three small-scale specimens obtained from the side wall of the profile and one full-scale specimen representing the complete cross-section of the profile. The measured material properties as listed in Table 1, were subsequently used as input parameters for the numerical models developed to simulate the behavior of the composite panels.

2.2 Specimen Dimensions and Configurations

The fabricated specimens had nominal dimensions of 1300 × 600 mm, with each specimen representing one of four distinct configurations. These dimensions were derived by scaling down a hypothetical unitized curtain wall panel with full-scale dimensions of 3900 × 1800 mm using a scale factor of 3. Variations between the specimen configurations were primarily attributed to differences in thickness and material composition. Table 2 provides a summary of the configurations, specimen thicknesses, and their corresponding specimen IDs.

As summarized in Table 2, the specimen “ALU-SIL-TG”, featuring an aluminium core bonded with silicone adhesive, served as the control sample. This configuration

Table 2. Summary of specimen configuration

Specimen ID	Glass face sheet type		Core	Adhesive	Total thickness (mm)
	Top	Bottom			
ALU-SIL-TG	Toughened	Toughened	Aluminium	Silicone	72.0
GFRP-SIL-TG	Toughened	Toughened	GFRP	Silicone	76.0
GFRP-EPX-TG	Toughened	Toughened	GFRP	Epoxy	65.0
GFRP-EPX-LG	Toughened	T. Laminated	GFRP	Epoxy	66.5

represents the materials most commonly used in glazed unitized curtain wall systems. In contrast, the specimen "GFRP-SIL-TG" replaced the aluminium core with a GFRP core while maintaining the use of the silicone adhesive, allowing for a direct comparison of the performance of aluminium and GFRP cores under similar bonding conditions.

The remaining two specimens, "GFRP-EPX-TG" and "GFRP-EPX-LG", both incorporated GFRP cores but were bonded with an epoxy-based adhesive. These configurations enabled a comparative analysis between silicone and epoxy adhesives, highlighting the influence of a stiffer bonding system on the structural performance of specimens with GFRP cores. This experimental design facilitates a comprehensive evaluation of the effects of core material and adhesive type on the behaviour of the specimens. Additionally, the "GFRP-EPX-LG" specimen incorporated a toughened laminated glass face sheet on the tensile face, distinguishing it from the other specimens, which all utilized fully toughened glass face sheets on both faces.

The fully toughened soda-lime glass face sheets used in the specimens had a nominal thickness of 10 mm with polished edges, manufactured in accordance with BS EN 755 [11] standards. The laminated glass face sheet employed in specimen "GFRP-EPX-LG" was composed of two 5 mm thick fully toughened glass layers laminated using a 1.52 mm thick PVB interlayer, meeting the requirements of BS EN 14449 [12] standards.

The pultruded GFRP square hollow section core, classified as a structural profile (E23), was supplied by Engineered Composites UK. The profile had nominal dimensions of 44 $\times$ 44 mm with a wall thickness of 6 mm. The aluminum core used in the "ALU-SIL-TG" specimen was extruded from 6063 alloy, featuring nominal dimensions of 40 $\times$ 40 mm with a wall thickness of 2 mm. The aluminum profile was mill-finished to enhance adhesion.

The sizing of the aluminum SHS section was carefully selected based on its flexural stiffness, ensuring compatibility with the flexural stiffness of the GFRP profiles. This selection criterion was critical to facilitate a meaningful comparison between the structural behaviors of the aluminum and GFRP-based specimens under identical loading conditions.

Two distinctly different bond line thicknesses were employed for the Dow Corning 995, a one-part, self-curing silicone structural glazing adhesive, and 3M ScotchWeld DP490, a two-part, self-curing epoxy adhesive. The silicone-based specimens employed a bond line thickness of 6 mm, as recommended by the manufacturer. This thickness was controlled using double glazing spacer tape, following industry standards for structural

silicone glazing. In contrast, the epoxy-based specimens featured a significantly thinner bond line of 0.5 mm, designed to achieve higher lap shear strength and optimize the structural performance of the bonded joint. This bond line thickness was controlled by placing small aluminum plates (0.5 mm thick) at the two corners of the GFRP core profile.

Before the application of the adhesive, all bonding surfaces were thoroughly cleaned with propan-2-ol alcohol to remove grease and dirt. For the silicone-based specimens, both glass face sheets were bonded simultaneously, following a method similar to double-glazing bonding technique commonly used in the industry. In contrast, for the epoxy-based specimens, the bonding process was conducted in two distinct stages. This approach allowed precise control of the bond line thickness, ensuring uniformity and of the bond. All specimens were cured for a minimum of 21 days prior to being tested (Fig. 1).

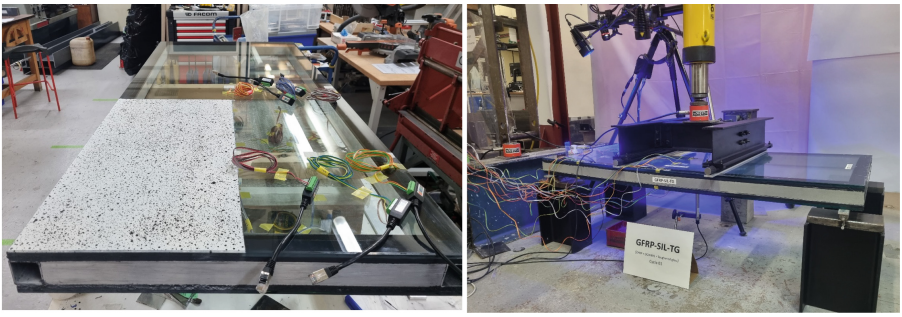

Fig. 1. Prepared specimen with data acquisition sensors (Left), Specimen under load (Right)

2.3 Data Acquisition Setup

To assess the structural behavior of the specimens under applied loading, a combination of strain gauges, Linear Variable Differential Transformers (LVDTs), and three-dimensional Digital Image Correlation (3D DIC) was employed. A total of 15 strain gauges were affixed to the outer surface of the glass face sheets. Specifically, six strain gauges were placed on the compression face sheet (top), while nine were positioned on the tensile face sheet (bottom). Given the symmetrical configuration of the specimens, strain gauges were strategically arranged to cover one-quarter of the specimen. This approach assumed that all quarters of the specimen would exhibit identical composite action and mechanical behavior.

To enable accurate stress distribution analysis and three-dimensional deformation measurements, a random speckle pattern with an average speckle size of 1.29 mm was applied to a 300 × 388 mm section of the top glass face sheet. The 3D DIC system captured high-resolution stress and deformation data, providing critical insights into the glass face sheet's behavior under loading.

An LVDT was placed at the mid-span of the bottom face sheet to measure vertical deflection. Additionally, two LVDTs were installed along the edges of the specimen to

monitor linear slippage between the glass face sheets and the structural hollow section (SHS) core along the long edge. This comprehensive instrumentation enabled detailed evaluation of the specimens' structural performance, including deflection behavior, stress distribution, and the degree of composite action.

2.4 Experimental Test Procedure

All four specimens were tested using a custom-modified test rig designed to accommodate their dimensions while replicating realistic boundary conditions. The specimens were supported at all four corners using 120 mm long steel rollers, simulating the support conditions typically encountered in unitized curtain wall systems. The load was applied using two steel rollers spanning the full width of the specimen, ensuring a uniform distribution across the specimen width, as illustrated in Fig. 2.

The loading was applied using a manually controlled hydraulic jack at a displacement-controlled rate of 1 mm/min until ultimate failure. Data recording was conducted at a frequency of 10 Hz using StrainSmart software, allowing for high-resolution monitoring of the structural response. This setup provided comprehensive data on load, deflection, and strain, which were essential for evaluating the performance and failure characteristics of the specimens under applied loading conditions.

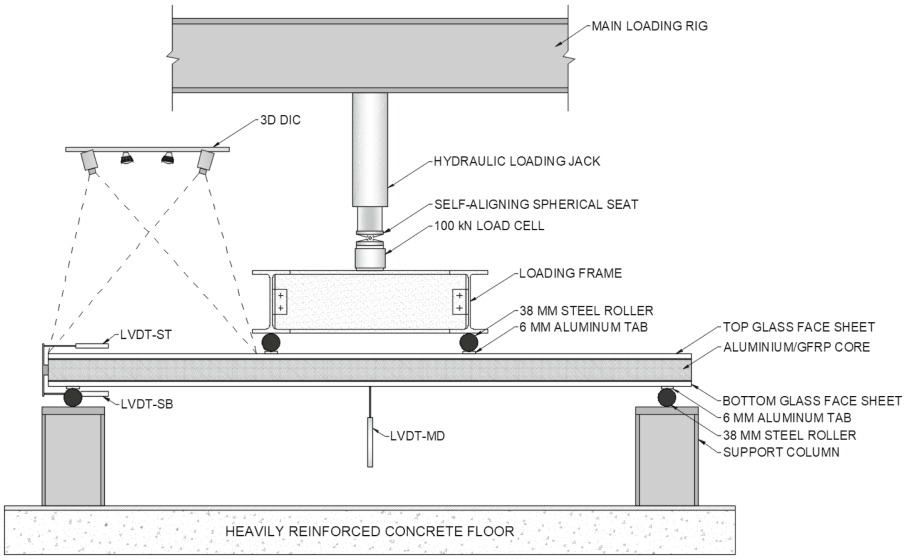

Fig. 2. Experimental set up

3 Numerical Simulation

Specimen "GFRP-EPX-TG" was simulated using a finite element model developed on ANSYS 2023 R2 Workbench. A quarter-section model was developed (Fig. 3 - Right), taking advantage of the specimen's double symmetry to optimize computational efficiency. Geometric details, such as glass fillet edges and the GFRP core's edge radius, were omitted to reduce computational time which did not compromise accuracy. All materials were assumed to behave in a linear elastic manner; therefore, no failure criteria or damage models were included in the simulation.

A hex-dominant mesh (HEX165) was applied, with a 3 mm mesh for the glass face sheets and GFRP core, and a 0.5 mm mesh for the adhesive layer. Boundary conditions at the supports restricted displacement along the Y-axis while allowing movement along the X and Z axes. The applied load was modeled as two-line pressures along the width, mimicking the experimental loading.

The finite element (FE) model was validated against experimental data by comparing deformation and stress distributions under applied loads of 40 kN and 90 kN. Mid-span deflections of the bottom glass face sheet obtained from the simulations closely matched experimental results, confirming the model's reliability. The validated model provided insights into the deformation and stress behavior of the composite specimen and is beneficial to simulate the behavior of actual size panels.

4 Results and Discussion

During the testing of the four specimens, the failure mechanisms were carefully observed and recorded. Table 3 summarizes the failure patterns for each specimen, providing valuable insights into their failure mechanisms. The distinct failure modes observed highlight the influence of varying material configurations and compositions. To ensure accurate identification of failure modes, slow-motion footage was utilized, allowing for detailed analysis of the failure progression and mechanisms. These observations are instrumental in understanding the structural performance and limitations of the different configurations under applied loads.

Table 3. Specimen failure patterns

Specimen ID	Failure pattern		
	1st failure	2nd failure	3rd failure
ALU-SIL-TG	Top glass	Bottom glass	Aluminium core
GFRP-SIL-TG	Bottom glass	Top glass	–
GFRP-EPX-TG	GFRP core	Top glass	Bottom glass
GFRP-EPX-LG	GFRP core	Top glass	Bottom glass

The failure mechanisms of the specimens varied significantly based on material configurations and adhesive systems. The "ALU-SIL-TG" specimen failed progressively,

with initial failure of the top glass face sheet, followed by the bottom glass face sheet, and ultimately chord-side failure of the aluminium core beneath the loading points was caused due to excessive deflections. Permanent deformations were observed upon unloading, indicating yielding in the core. In the “GFRP-SIL-TG” specimen, failure began in the bottom glass face sheet, followed by the top face sheet, while the GFRP core remained intact with no visible damage.

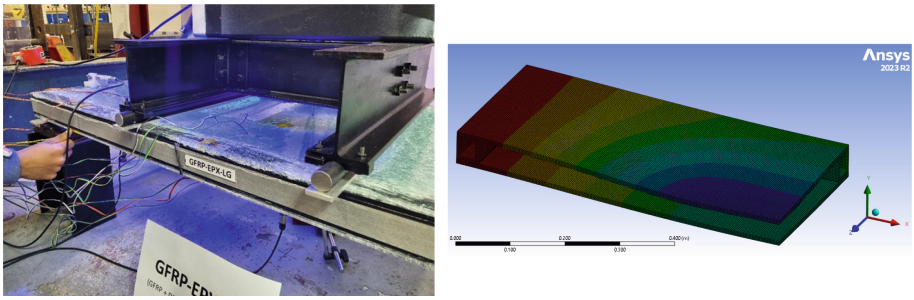

Fig. 3. Specimen "GFRP-EPX-LG" upon failure (Left), Quarter symmetrical FE model of "GFRP-EPX-TG” (Right)

The epoxy-bonded specimens, “GFRP-EPX-TG” and “GFRP-EPX-LG”, exhibited different failure patterns. Horizontal shear failure occurred along the long edge of the GFRP core, initiating between a support point and a loading point and propagating toward the opposite support. Both glass face sheets failed instantaneously, with the top (compression) face sheet failing first, followed closely by the bottom (tensile) face sheet. It remains uncertain whether the failure of the tensile face sheet was influenced by the impact from shards of the top glass face sheet. These results shows that the epoxy adhesive resulted in a better load transfer between the elements, and that the two glass face sheets absorbed majority of the loads, which resulted in GFRP core’s failure.

The load vs. mid-span deflection relationships of the panels is shown in Fig. 4, with loads corrected to account for the loading frame dead weight. The figure also shows the 1st, 2nd and 3rd failure point of the specimen with reference to Table 3 presented above. The deformation data obtained from the FE model for specimen “GFRP-EPX-TG” is also presented in the same graph.

Silicone-based specimens (“ALU-SIL-TG” and “GFRP-SIL-TG”) failed at significantly lower loads compared to epoxy-based specimens (“GFRP-EPX-TG” and “GFRP-EPX-LG”). The “ALU-SIL-TG” specimen sustained only 25% of the average load borne by the epoxy-based specimens, while the “GFRP-SIL-TG” specimen achieved 34%. Although the reduced height of the “ALU-SIL-TG” specimen may have contributed to the lower failure load compared to “GFRP-SIL-TG”. Silicone-based specimens exhibited mid-span deflections over 430% greater than epoxy-based specimens at failure, highlighting the superior stiffness of epoxy-bonded panels due to its efficient load transfer.

The epoxy-bonded specimens exhibited pronounced shear lag effects; a phenomenon linked to the inherent stiffness of the epoxy adhesive layer. This stiffness facilitates abrupt

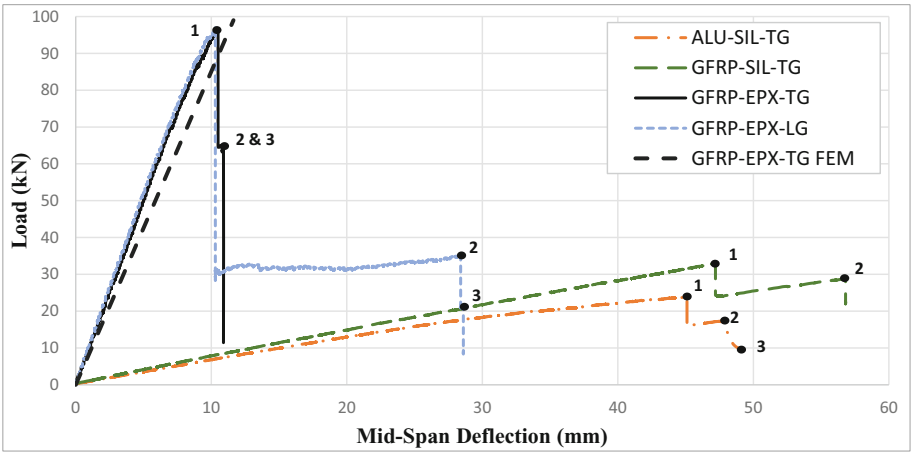

Fig. 4. Load Vs. Mid-span deflection of specimens

shear transfer near the bonded regions, leading to localized stress concentrations. These concentrations diminish with distance from the bonded area, resulting in significant shear lag. Conversely, the silicone adhesive layer, owing to its greater flexibility, accommodates larger movements and promotes a more uniform stress distribution, thereby minimizing the extent of shear lag.

Therefore, it is essential to develop methods which could effectively reduce the shear lag effects as this would further optimize the structural performance as well as reduce the chance of premature failure.

5 Conclusion and Future Research

This study investigated the flexural behavior of adhesively bonded composite façade panels, comprising GFRP cores with glass face sheets and an aluminium-core specimen. The panels were bonded with either silicone or epoxy-based adhesives and subjected to flexural loading under boundary conditions replicating real-world applications. Key findings include:

1. Composite Action and Load Capacity: Epoxy-bonded specimens exhibited superior composite action, achieving failure loads more than four times higher than silicone-bonded specimens, along with 75% reduced mid-span deflections at failure.
2. Failure Modes: GFRP cores in silicone-bonded specimens sustained no failure, while epoxy-bonded specimens experienced horizontal shear failure in the GFRP core.
3. Shear Lag Effect: Strain distribution analysis using strain gauges and 3D DIC revealed a more pronounced shear lag effect in epoxy-bonded specimens compared to their silicone-bonded counterparts.
4. Deformation Patterns: Epoxy-bonded specimens exhibited non-uniform (S-shaped) deformation along their length, whereas silicone-bonded specimens showed uniform deformation.

It is important to note that future research should explore the long-term performance of composite panels under environmental and thermal conditions, as well as their behavior under dynamic and impact loading scenarios. Additionally, optimizing adhesive properties and hybrid core configurations can further enhance structural efficiency and application potential.

Acknowledgments. The authors would like to express their heartfelt gratitude to Engineered Composites UK for their generous provision of the pultruded GFRP sections used in this research. Their invaluable support played a crucial role in advancing the study of composite materials and their practical applications.

References

1. Louter, C.: Adhesively bonded reinforced glass beams. Heron. **52**, 31–58 (2007)
2. Valarinho, L., Correia, J.R., Branco, F.A.: Experimental study on the flexural behaviour of multi-span transparent glass–GFRP composite beams. Constr. Build. Mater. **49**, 1041–1053 (2013). https://doi.org/10.1016/j.conbuildmat.2012.11.024
3. Pascual, C., Montali, J., Overend, M.: Adhesively-bonded GFRP-glass sandwich components for structurally efficient glazing applications. Compos. Struct. **160**, 560–573 (2017). https://doi.org/10.1016/j.compstruct.2016.10.059
4. Ranaweera, D., Zafari, B., Overend, M.: Structural Performance of adhesively bonded glass GFRP sandwich beams. In: Challenging Glass Conference Proceedings, Delft, vol. 9 (2024)
5. Nhamoinesu, S., Overend, M.: The mechanical performance of adhesives for a steel-glass composite façade system. In: Challenging Glass 3 – Conference on Architectural and Structural Applications of Glass (2012)
6. Pascual, C., Nhamoinesu, S., Overend, M.: The flexural response of large scale steel-framed composite glazing panels. Glass Struct. Eng. **4**, 199–207 (2019). https://doi.org/10.1007/s40940-019-00096-4
7. Gargallo, M., Cordero, B., Garcia-Santos, A.: Material selection and characterization for a novel frame-integrated curtain wall. Materials **14**, 1896 (2021). https://doi.org/10.3390/ma14081896
8. Cobb, F.: Structural Engineers Pocket Book Eurocodes. CRC Press, Taylor & Francis Group, Boca Raton (2015)
9. Dow Chemical Company: DOWSIL^{TM} 995 Silicone Structural Sealant Behavioral Data Sheet (63-6668-01) (2018)
10. ASTM International: ASTM D3171-11 Standard Test Methods for Constituent Content of Composite Materials (2011)
11. BSI: BS EN 755: Aluminium and aluminium alloys. Extruded rod/bar, tube and profiles, London (2016)
12. BSI: BS EN 14449:2005: Glass in building—Laminated glass and laminated safety glass—Evaluation of conformity/Product standard, London (2005)